

MODELING INJECTION MOULDING PARAMETERS FOR FLEXURAL RESPONSES OF BIO-FIBRE FILLED POLYMER COMPOSITES

ABSTRACT

This work is on modeling injection moulding parameters for a bio-fibre filled polymer composite in this case its flexural response. Mercerization and acetylation treatments were applied in surface modification of the bio-fibre. These fibres were ground and sieved into three particle sizes and applied as fillers in the matrix (high density polyethylene). The composites were compounded applying Taguchi robust design of experiment considering seven injection moulding parameters and one non-machine parameter being volume fraction of the reinforcing fibre. An L_{18} orthogonal array at mixed levels was adopted for the experiment and response evaluation. Analysis on the composites of the three particle sizes show that volume fraction was control factor that has the highest influence on the flexural properties of the composites. Analysis of variance (ANOVA) showed that the independent variables in the models can explain over 80% of the response, hence indicating response model fit. The generated predictive models indicated a goodness of fit, hence can comfortably predict the response.

Keywords: Bio-fibre, Composites, Flexural Response, Modeling, Taguchi Robust Design

1. INTRODUCTION

Flexural test measures the force required to bend a beam under three or four point loading conditions. The data is often used to select materials for parts that will support loads without flexing. Flexural strength represents the highest stress experienced within a material at its moment of yield. Flexible materials such as elastomers have lower flexural values than fibre reinforced engineering polymers used as metal substitutes such as the plantain pseudo-stem fibre reinforced high density polyethylene (PFRHDPE) developed by this research. However, this research is motivated by the fact that the common practice of considering a natural fibre as an undesirable waste, results in its burning or disposed on landfills and contributing to environmental pollution. Therefore, in order to preserve the environment, it is necessary to find economically feasible solution to the increasing amount of natural fibre wastes. This can be achieved through the understanding of natural fibres as recyclable materials, which could be used for different applications ranging from handicrafts to reinforcement elements for composites [1].

Fibre reinforced polymeric based composite materials are being used for many life applications, such as; automotive, sporting goods, marine, electrical, industrial, construction, household appliances, oil and gas pipelines and accessories, etc. [2]. These engineering materials offer many benefits ranging from high strength, light weight, water resistance, chemical resistance, high durability, electrical resistance, fire resistance to corrosion resistance. However, the properties and performance of fibre composites can be engineered according to the requirements and thus cost effective in most usage and applications [3], [4]; [5], [6].

The underlying principle in fibre composites is to utilize fibres as reinforcement in matrix of resin. The fibres usually provide the greatest share of strength while resin provides binding to the fibers. Ticoalu, Aravinthan, and Cardona [4] state that fibres themselves cannot be used to sustain actual loads, hence, resin is used to bind and protect the fibres. The properties of fibre composites can be tailored to achieve the desired end product depending on the type of fibres, type of resin, the proportion of fibre-resin and the type manufacturing process [7], [8].

Pipeline integrity management program (PIMP) which is a program through which oil and gas companies manage and control the problem of corrosion along pipeline and piping systems has become extra ordinarily expensive. Corroding infrastructure is costing developed and developing nations alike trillions of dollars annually in repairs and replacement costs. A recent estimate of the worldwide direct cost of corrosion- for prevention as well as repairs and replacement exceeded \$1.8 trillion, or 3 to 4 percent of the Gross Domestic Product (GDP) of industrialized countries [9]. Composites are actually finding application in the oil and gas industry, onshore and offshore. The most significant advances have been made in the areas of pipe works and fluid handling, driven by light weight and corrosion resistance compared to metals. Expansion is therefore expected to continue into all sectors of oil and gas industry [10],[11],[12].

The plantain pseudo-stem particulate filled high density polyethylene composites produced from this research is designed for application in oil and gas pipeline transport system. Objective of this research is to find an alternative material for application in place of corroding carbon based steel pipes to mitigate against corrosion as pipeline material are unavoidably operated or applied in pro-corrosion environments. This informs the mechanical tests to which these composites were subjected to, of which flexural response is one of them.

2. MATERIALS AND METHODOLOGY

2.1 Fibre Surface Modification

A major disadvantage associated with the use of natural fibres as reinforcements in composites is their high hydrophilic nature which leads to low mechanical properties and sometimes delamination. This reduction in mechanical properties cannot be unconnected to poor interfacial bonding the hydrophobic matrices and the hydrophilic natural fibres. Therefore, to enhance the effective interfacial bonding between fibre and matrix, the fibre surface needs to be chemically modified [13],[14],[15]. Mercerization is one of the treatments and fibre modification technique that was adopted in this research. Mercerization increases the number of possible reactive sites, allows better fibre wetting and gets an effect on the chemical composites of the fibres. Mercerization also takes out certain portion of hemicelluloses, lignin, pectin, wax and oil covering the fibres, as a result, the fibre surface becomes more uniform due to the elimination of micro voids and thus stress transfer capacity between the ultimate cells improves [16].

Acetylation is the second fibre surface modification practice this research engaged in the development of its fibre materials, hence we shall further review its applications and findings in literature. Moreover, acetylation can reduce the hygroscopic nature of natural fibres and increase the dimensional ability of composites. It was used in surface treatment of fibres for use in fibre reinforced composites by researchers. Mishra, et al [17] reported an improvement in fibre-matrix adhesion for an alkali treated sisal fibre soaked in glacial acetic acid and later in acetic anhydride containing one drop of H_2SO_4 for 5mins. Bledzki and Gassan [18] in their work reported a reduction of about 50% of moisture uptake for acetylated jute fibres and up to 65% for acetylated pine fibres.

2.2 Application of Taguchi Robust Design Analysis

In designing the experimental runs or processes for this research we applied the Taguchi design of experiment (DOE). The DOE consists of 8 (eight) controllable parameters or factors or variables at 3-levels of design (Table 1) for which we choose the L_{18} orthogonal array. Though the DOE has 8 factors and three levels, one would have simply gone for the L_{27} array but this would certainly have increased the cost of the experiment, hence the adoption of a mixed $L_{18} (2^1 \times 3^7)$ array.

Meanwhile, signal-to-noise ratio (S/N) is an important quality characteristics of Taguchi DOE which we will compute using the Larger the Better position as in equation (1);

$$S/N = -10 \left[\frac{1}{n} \left(\frac{1}{y_1^2} + \frac{1}{y_2^2} + \dots + \frac{1}{y_n^2} \right) \right] \quad (1)$$

Where $y_1, y_2 \dots y_n$ are the responses for a trial condition repeated n times and S/N ratio of each response will be computed for each trial. The main effects of factors along with their percentage contribution will be computed. The difference between highest and lowest values of S/N ratio or means will be used to calculate the delta values. The delta values along with percentage contributions are used to rank the individual factor [19]. This Taguchi analysis usually produce a first-order model. The first order model is likely to be appropriate when the experimenter is interested in approximating the true response surface

over a relatively small region of the independent variable space in a location where there is little curvature in f . For the case of two independent variables, the first-order model in terms of the coded variables is;

$$y = \beta_0 + \beta_1x_1 + \beta_2x_2 \quad (2)$$

The form of the first-model in equation (2) is sometimes called a 'main effects model' because it includes only the main effects of the two variables x_1 and x_2 . If there is an interaction between these variables, it can be added to the model easily as follows;

$$y = \beta_0 + \beta_1x_1 + \beta_2x_2 + \beta_{12}x_1x_2 \quad (3)$$

This is the first-order model with interaction, but adding the interaction term introduces curvature into the response function. Often the curvature in the true response surface is strong enough that the first order model (even with the interaction term included) is inadequate.

Table 1: Design Factors and Levels

S/NO	DESIGN FACTORS	LEVELS		
		1	2	3
F1	Screw Speed (SS) rpm	20	40	40
F2	Volume Fraction (V_{fr}) %	10	30	50
F3	Barrel Temperature (TB) °C	150	200	250
F4	Mold Temperature (TM) °C	30	35	40
F5	Injection Pressure (IP) MPa	70	87.5	105
F6	Holding Pressure (HP) MPa	56	70	84
F7	Back Pressure (BP) MPa	0.4	0.8	1.2
F8	Clamping Force (CF) tons	133	140	147

Table 2: Populated Taguchi L_{18} ($2^1 \times 3^7$) Orthogonal array

Experiment	SS (rpm)	V_{fr} (%)	TB (°C)	TM (°C)	IP (MPa)	HP (MPa)	BP (MPa)	CF (tons)
1	20	10	150	30	70	56	0.4	133
2	20	10	200	35	87.5	70	0.8	140
3	20	10	250	40	105	84	1.2	147
4	20	30	150	30	87.5	70	1.2	147
5	20	30	200	35	105	84	0.4	133
6	20	30	250	40	70	56	0.8	140
7	20	50	150	35	70	84	0.8	147
8	20	50	200	40	87.5	56	1.2	133
9	20	50	250	30	105	70	0.4	140
10	40	10	150	40	105	70	0.8	133
11	40	10	200	30	70	84	1.2	140
12	40	10	250	35	87.5	56	0.4	147
13	40	30	150	35	105	56	1.2	140
14	40	30	200	40	70	70	0.4	147
15	40	30	250	30	87.5	84	0.8	133
16	40	50	150	40	87.5	84	0.4	140
17	40	50	200	30	105	56	0.8	147
18	40	50	250	35	70	70	1.2	133

Most importantly, Taguchi DOE and optimization technique has shortcomings as it only identifies the linear effect of factors, while ignoring the quadratic effect and little or no interaction effect.

2.3 Composite Development

The plantain pseudo stem particulate reinforced high density polyethylene composites developed in this research were compounded using three different sieve sizes of the fibre particulate designated as particle sizes (PS1, PS2, and PS3). To enhance wettability between matrix and filler, two compatibilizers or

coupling agents of grafted maleic anhydride polyethylene were also employed. However, through the tests carried out composites of compatibilizer 09 showed better mechanical properties than '08, hence all analysis will be based on the results obtained from those of '09. It has been foregone established that compatibilized reinforced polymer composites have better properties than neat reinforced polymer composites used as control, therefore, it is not necessary to analyze the results of the control.

2.4 Experiments and Flexural Tests

Flexural tests on the developed PFRHDPE materials were conducted in accordance with ASTM D790 standards specifications. During the flexural tests, it was observed that the PFRHDPE materials could not failed under flexural loading but continue bend to a point where more strain did not show further significant effect on the material. The flexural strength of the material was therefore established at this point of no strain effect in accordance with the stipulated standard. However, flexural strength of an engineering material is the maximum flexural stress sustained by a test specimen during a bending test. Some materials like the one under study, that do not break at certain strains may give a load deflection curve that shows a point at which the load does not increase with increase in strain i.e. yield point. This flexural strength can be calculated applying the following relation:

$$\sigma_f = \frac{3YL}{2bd^2} \quad (4)$$

Where σ_f = Maximum flexural stress (MPa); Y = Yield point load (N); L = Support span mm (in); b = Width of specimen mm (in); d = Depth of specimen mm (in).

The results obtained from the flexural tests for compatibilizer 09 of the three particle sizes were reported using the design matrix as in Table 3.

3. RESULTS AND DISCUSSION

Results obtained from the flexural experiments as mentioned earlier were presented in the form of design matrix of Table 3 and every analysis was carried out employing these design matrices.

Table 3: Experimental Design Matrix of Taguchi Analysis for Flexural Responses of Particle Size 1

Exp. Runs	SS (rpm)	Vfr (%)	TB (°C)	TM (°C)	IP (MPa)	HP (MPa)	BP (MPa)	CF (tons)	Response (MPa)
1	20	10	150	30	70	56	0.4	133	78.63
2	20	10	200	35	87.5	70	0.8	140	76.92
3	20	10	250	40	105	84	1.2	147	78.39
4	20	30	150	30	87.5	70	1.2	147	87.45
5	20	30	200	35	105	84	0.4	133	102.88
6	20	30	250	40	70	56	0.8	140	90.88
7	20	50	150	35	70	84	0.8	147	69.81
8	20	50	200	40	87.5	56	1.2	133	76.92
9	20	50	250	30	105	70	0.4	140	68.34
10	40	10	150	40	105	70	0.8	133	75.20
11	40	10	200	30	70	84	1.2	140	68.34
12	40	10	250	35	87.5	56	0.4	147	76.92
13	40	30	150	35	105	56	1.2	140	94.31
14	40	30	200	40	70	70	0.4	147	97.74
15	40	30	250	30	87.5	84	0.8	133	90.86
16	40	50	150	40	87.5	84	0.4	140	94.31
17	40	50	200	30	105	56	0.8	147	82.06
18	40	50	250	35	70	70	1.2	133	94.31

3.2 Taguchi DOE Analysis of Flexural Responses

Experimental design matrix was formed for the Flexural response of particle size 1 (Table 3), changing only the mean response with that for two other particle sizes, the experimental matrices were formed for

other particle size results and analyzed using Minitab 17 version. Therefore, from this matrix every other analysis was performed, and results reported as follows. The first approach to the analysis included interaction effects, as this is at the point of curvature for Taguchi robust design, the ANOVA results showed a point of saturation with zero degree of freedom for error effect. This resulted to a situation where F and P values were not evaluated due to saturation of model, hence, we carried out a model re-fit in all cases of the particle sizes. The response tables for all particle size for signal to noise ratio (larger is better) and means followed the same sequence.

3.2.1 Analysis for Flexural Response Particle Size 1

Table 4: Response Table for Signal-to-Noise Ratio (Larger is better) for Flexural Response Particle Size 1

<i>Level</i>	<i>SS (rpm)</i>	<i>Vfr (%)</i>	<i>TB (°C)</i>	<i>TM (°C)</i>	<i>IP (MPa)</i>	<i>HP (MPa)</i>	<i>BP (MPa)</i>	<i>CF (tons)</i>
<i>1</i>	38.12	37.58	38.36	37.93	38.32	38.38	38.64	38.68
<i>2</i>	38.63	39.45	38.41	38.59	38.44	38.34	38.12	38.21
<i>3</i>		38.09	38.35	38.60	38.35	38.39	38.35	38.23
<i>Delta</i>	0.51	1.88	0.06	0.67	0.12	0.05	0.52	0.47
<i>Rank</i>	4	1	7	2	6	8	3	5

Table 5: Response Table for Means for Flexural Response Particle Size 1

<i>Level</i>	<i>SS (rpm)</i>	<i>Vfr (%)</i>	<i>TB (°C)</i>	<i>TM (°C)</i>	<i>IP (MPa)</i>	<i>HP (MPa)</i>	<i>BP (MPa)</i>	<i>CF (tons)</i>
<i>1</i>	81.14	75.73	83.28	79.28	83.28	83.29	38.64	86.47
<i>2</i>	86.01	94.02	84.14	85.86	83.90	83.33	38.12	82.18
<i>3</i>		80.96	83.28	85.57	83.53	84.10	38.35	82.06
<i>Delta</i>	4.87	18.29	0.86	6.58	0.61	0.81	0.52	4.40
<i>Rank</i>	4	1	7	2	6	8	3	5

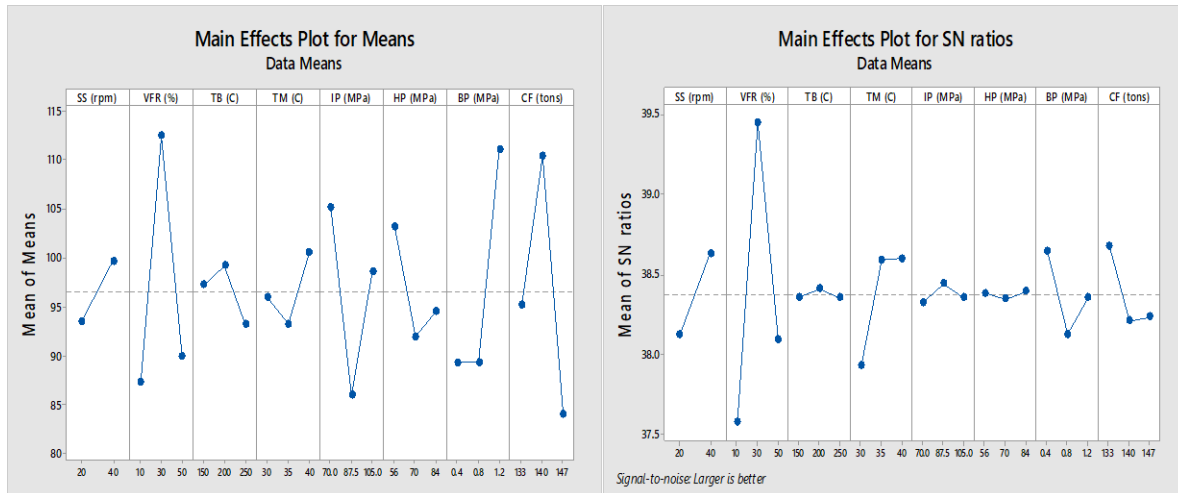


Fig. 1: Main Effects Plot of Signal-to-Noise (Larger is Better) for Flexural Response Particle Size 1

Fig. 2: Main Effects Plot of Means for Flexural Response Particle Size 1

The response tables (Tables 4 and 5) are those of signal-to-noise ratios and means analysis for the re-fit model. The ranks in these response tables show or indicate that volume fraction (Vfr) of Fibre has the greatest influence on Flexural response of particle size 1. This is followed by the mould temperature (TM) in Rank 2 and back pressure (BP) as rank 3.

ANOVA analysis result for the re-fit produced the coefficient of determination (R^2) of 75.4% and 77.5% for both S/N ratio and mean respectively. The main effect plots for S/N ratios and that of Means (Figs. 1 and 2 respectively) indicated the same outcome of optimum. They showed that the optimal flexural strength of this particle size is produced at the factor levels combination of; 40rpm Screw Speed, 30% Volume Fraction of fibre, 200°C Barrel Temperature, 40°C Mould Temperature, 87.5MPa Injection Pressure, 84MPa Holding Pressure, 0.4MPa Back Pressure, and 133tonnes Clamping Force.

The main effect plots, ranks of factors, values of sum of squares from ANOVA Tables are all in conformity with coefficients of the linear models produced for the response. The absolute value of these coefficients shows the importance of each factor to the response, hence, volume fraction still remains the best factor of influence.

The estimated model of coefficients for S/N ratios for flexural response particle size 1 is obtained as,

$$\begin{aligned}
 Flexural_{PS1} = & 38.3736 - 0.2557SS - 0.7976Vfr + 1.0782Vfr - 0.0183TB + 0.0373TB - 0.4429TM \\
 & + 0.2179TM - 0.0494IP + 0.0691IP + 0.0091HP - 0.0292HP + 0.2706BP \\
 & - 0.2498BP + 0.3034CF \\
 & - 1.1637CF
 \end{aligned} \tag{5}$$

The estimated model of coefficients for Means of PS1 is,

$$\begin{aligned}
 Flexural_{PS1} = & 83.5706 - 2.4350SS - 7.8372Vfr + 10.4494Vfr - 0.2856TB + 0.5728TB - 4.2906TM \\
 & + 2.2878TM - 0.2856IP + 0.3261IP - 0.2839HP - 0.2439HP + 2.8994BP \\
 & - 2.6156BP + 2.8961CF \\
 & - 1.3872CF
 \end{aligned} \tag{6}$$

3.2.2 Analysis for flexural response particle size 2

Table 6: Response Table for Signal-to-Noise Ratio (Larger is better) for Flexural Response Particle Size 2

Level	SS (rpm)	Vfr (%)	TB (°C)	TM (°C)	IP (MPa)	HP (MPa)	BP (MPa)	CF (tons)
1	39.65	37.40	39.33	39.33	39.20	39.19	39.03	39.08
2	38.83	39.80	39.29	39.03	39.33	39.31	39.45	38.98
3		40.52	39.09	39.36	39.18	39.22	39.23	39.65
Delta	0.82	3.12	0.24	0.32	0.15	0.12	0.42	0.67
Rank	2	1	6	5	7	8	4	3

Table 7: Response Table for Means for Flexural Response Particle Size 2

Level	SS (rpm)	Vfr (%)	TB ($^{\circ}C$)	TM ($^{\circ}C$)	IP (MPa)	HP (MPa)	BP (MPa)	CF (tons)
1	97.77	74.14	94.43	94.39	92.68	92.72	90.47	91.04
2	88.24	98.56	93.58	90.76	94.23	93.66	95.37	90.11
3		106.31	91.00	93.86	92.10	92.63	93.17	97.86
Delta	9.52	32.17	3.43	3.63	2.13	1.02	4.90	7.76
Rank	2	1	6	5	7	8	4	3

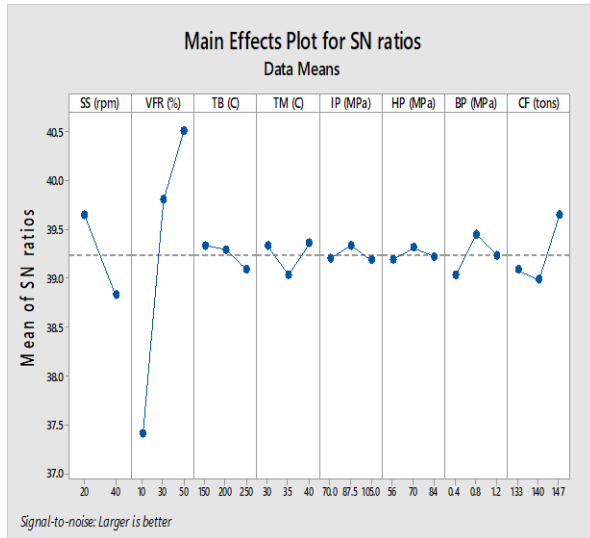


Fig. 3: Main Effects Plot of Signal-to-Noise (Larger is Better) for Flexural Response Particle Size 2

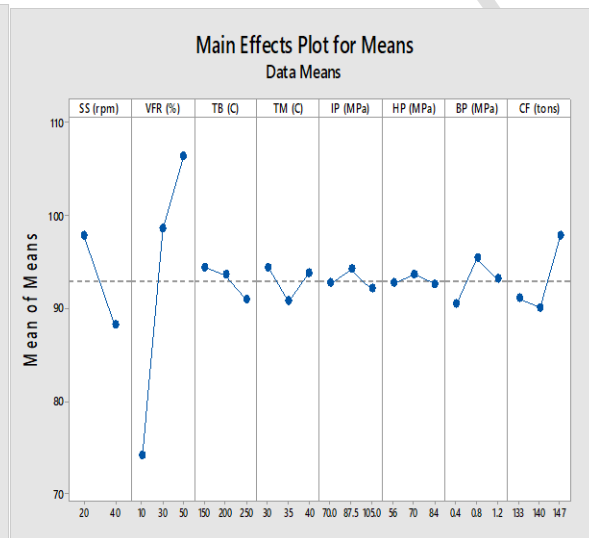


Fig. 4: Main Effects Plot of Means for Flexural Response Particle Size 2

The response tables for signal-to-noise ratios and mean (Tables 6 and 7) for the re-fit model showed the same results about variables' rank as Volume Fraction (Vfr) is Rank 1, Screw Speed (SS) is Rank 2, Clamping Force (CF) is Rank 3 and so on. The ranking was according to each variable's influence on the Flexural strength of particle size 2.

Analysis of variance for signal-to-noise reported a 91.0% coefficient of determination (R^2) while the ANOVA for means for same refit reported R^2 of 89.9%. The main effect plots of Figs 3 and 4 (signal-to-noise ratios and means) predicted that an optimum Flexural strength value can be obtained for particle size 2 at the following factors levels combination; 20rpm Screw Speed, 50% Volume fraction, 150 $^{\circ}C$ Barrel Temperature, 40 $^{\circ}C$ Mould Temperature, 87.5MPa Injection Pressure, 70MPa Holding Pressure, 0.8MPa Back Pressure, and 147tonnes Clamping Force.

The main effect plots, ranks of factors, values of sum of squares from ANOVA Tables are all in conformity with coefficients of the linear models produced for the response. The absolute value of these coefficients shows the importance of each factor to the response, hence, volume fraction still remains the best factor of influence.

The estimated model of coefficients for S/N ratios for particle size 1 is obtained as,

$$\begin{aligned}
 Flexural_{ps2} = & 39.2381 + 0.4110SS - 1.8397Vfr + 0.5603Vfr + 0.0929TB + 0.0547TB + 0.0896TM \\
 & - 0.2072TM - 0.0375IP + 0.0917IP - 0.0518HP + 0.0700HP - 0.2084BP \\
 & + 0.2118BP - 0.1545CF \\
 & - 0.2560CF
 \end{aligned} \tag{7}$$

The estimated model of coefficients for Means is,

$$\begin{aligned}
 Flexural_{ps2} = & 93.0033 + 4.7622SS - 18.8617Vfr + 5.5517Vfr + 1.4300TB + 0.5717TB + 1.3883TM \\
 & - 2.2450TM - 0.3250IP + 1.2250IP - 0.2850HP + 0.6533HP - 2.5317BP \\
 & + 2.3700BP - 1.9600CF \\
 & - 2.8983CF
 \end{aligned} \tag{8}$$

3.2.3 Analysis of flexural response particle size 3

Table 8: Response Table for Signal-to-Noise Ratio (Larger is better) for Flexural Response Particle Size 3

Level	SS (rpm)	Vfr (%)	TB ($^{\circ}$ C)	TM ($^{\circ}$ C)	IP (MPa)	HP (MPa)	BP (MPa)	CF (tons)
1	40.09	37.82	39.75	39.82	39.93	39.83	40.08	39.61
2	39.50	40.19	39.60	39.83	39.91	39.65	39.63	39.86
3		41.37	40.04	39.74	39.54	39.92	39.68	39.93
Delta	0.58	3.55	0.44	0.10	0.39	0.27	0.45	0.32
Rank	2	1	4	8	5	7	3	6

Table 9: Response Table for Means for Flexural Response Particle Size 3

Level	SS (rpm)	Vfr (%)	TB ($^{\circ}$ C)	TM ($^{\circ}$ C)	IP (MPa)	HP (MPa)	BP (MPa)	CF (tons)
1	101.90	78.43	99.41	99.41	100.84	98.84	102.27	97.41
2	96.71	102.31	96.80	99.37	100.23	98.23	97.94	100.23
3		117.18	101.70	99.13	96.84	100.84	97.70	100.27
Delta	5.20	38.75	4.90	0.29	4.00	2.61	4.57	2.86
Rank	2	1	3	8	5	7	4	6

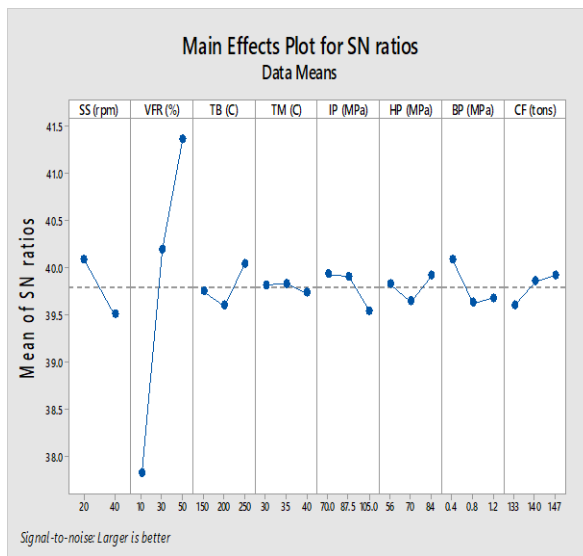


Fig. 5: Main Effects Plot of Signal-to-Noise (Larger is Better) for Flexural Response Particle Size 3

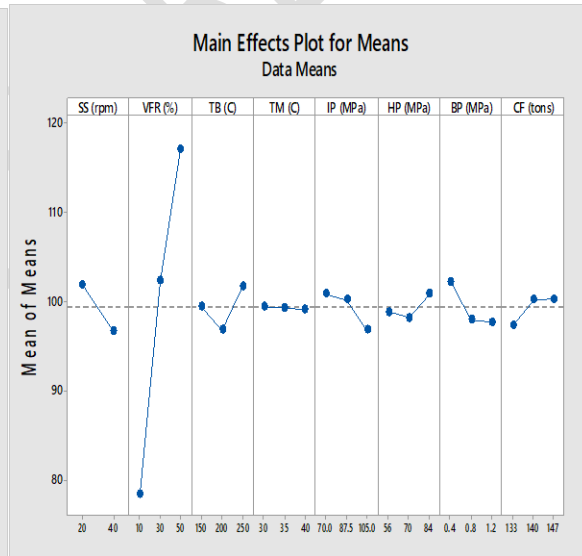


Fig. 6: Main Effects Plot of Means for Flexural Response Particle Size 3

Tables 7 and 8 are response tables for signal-to-noise ratios and for means respectively. The results of these response tables showed that, for signal-to-noise ratios the variable or factor Volume Fraction is Rank 1, with Screw Speed in Rank 2, while Back Pressure came up to Rank 3. But the tables of means show that the Barrel Temperature is Rank 3 instead of Back Pressure.

Analysis of variance (ANOVA) results of S/N ratios and means analyses produced coefficients of determination (R^2) of 91.3% and 93.5% respectively. Moreover, the main effects plot for signal-to-noise ratios and means (Figs. 5 and 6) produced the optimum factor levels for obtaining optimal Flexural strength at; 20rpm screw speed, 50% volume fraction, 250 $^{\circ}$ C barrel temperature, 35 $^{\circ}$ C mould temperature, 70MPa injection pressure, 84MPa holding pressure, 0.4MPa back pressure, and 147tonnes clamping force. In the same token, the main effect plots, ranks of factors, values of sum of squares from ANOVA Tables are all in conformity with coefficients of the linear models produced for the response. The

absolute value of these coefficients shows the importance of each factor to the response, hence, volume fraction still remains the best factor of influence.

The estimated model of coefficients for S/N ratios is obtained as,

$$\begin{aligned} Flexural_{PS3} = & 37.5041 + 0.0903SS - 1.8302Vfr + 2.0526Vfr - 0.0567TB - 0.3749TB + 0.3348TM \\ & - 0.4340TM - 0.1671IP - 0.3219IP - 0.0607HP + 0.3493HP + 0.7524BP \\ & - 1.0926BP - 0.4674CF \\ & + 0.4092CF \end{aligned} \quad (9)$$

The estimated model of coefficients for Means is,

$$\begin{aligned} Flexural_{PS3} = & 76.9400 + 0.6614SS - 15.4322Vfr + 18.2982Vfr + 0.2205TB - 2.8660TB \\ & + 2.4250TM - 2.8660TM - 2.2047IP - 2.8658IP - 0.8817HP - 1.5433HP \\ & + 6.3932BP - 8.8183BP - 4.1887CF \\ & + 4.4092CF \end{aligned} \quad (10)$$

4. CONCLUSION

The following conclusions are drawn from the research, thus:

1. Taguchi robust design approach in this work was able to develop predictive models that are fit in explaining the relationships between the injection moulding parameters that actually affect the compounding of PFRHDPE composites thus produced.
2. The response tables of signal-to-noise ratio and that of the means showed that fibre volume fraction (V_{fr}) has the greatest influence or effect on the flexural strength of the three particle sizes of fillers.
3. For optimum flexural strength to be achieved at material formation for each particle size, the analysis through the main effect plots was able to give the optimal parametric setting that could yield the best flexural property.
4. Analysis of variance (ANOVA) showed that the independent variables in the models can explain over 80% of the response, hence indicating response model fit.
5. The analysis produced estimated model coefficients that expressed conformity with all foregone inferences drawn from preceding analytical results.

REFERENCES

1. Schuh T, Gayer U. Automotive applications of natural fibre composites: Benefits for the environment and competitiveness with man-made materials. In: Leao, A.L., Carvalho, F.X., Frollini, E. (Ed). Lignocellulosic Plastics Composites, Sao Paulo. 1997; 181-195.
2. Ihueze CC, Obuka SPN. A review of corrosion and corrosion schemes for metal and composite oil and gas Systems: Management and development. Journal of Advanced Materials. 2011;43(2):35-54. Society for the Advancement of Material and Process Engineering, California, U.S.A.
3. Ihueze CC, Obuka SPN. (2016). Engineered composite materials and natural fibres: Design and manufacture (A review). IOSR Journal of Mechanical and Civil Engineering. 2016;13(3):86-93.
4. Ticoalu A, Aravinthan T, Cardona F. A review of current developments in natural fibre composites for structural and infrastructural applications. Southern Region Engineering Conference, University of Southern Queensland, Toowoomba, Australia; 2010.
5. Humphreys MF. Development and structural investigation of monocoque fibre composite trusses. Doctor of Philosophy, School of Civil Engineering, Queensland University of Technology, Brisbane; 2003.

6. Aravinthan T, Omar T. Fibre composite windmill structure- challenges in the design and development. In: Proceedings of Fourth International Conference on FRP Composites in Civil Engineering, Zurich, Switzerland; 2008
7. Rowell RM. Natural fibres: Types and properties, in properties and performance of natural fibre composites. K. Pickering, Ed., ed Cambridge: Woodhead Publishing Limited; 2008.
8. O'Donnell A, Dweib M, Woll R. Natural fibre composites with PHnt-cel based resin. Composites Sciences and Technology. 2004; 64:1135-1145.
9. Lieser MJ, Xu J. Composites and the future of society: Preventing a legacy of costly corrosion with modern materials. Owens Corning, Ohio, USA; 2010.
10. Composite Materials for Offshore Operations: Proceedings of the First International Workshop, Houston, Texas, October 26-28th 1993.
11. Gibson AG. The cost effective use of fibre reinforced composites offshore. Centre for Composite Materials Engineering, University of Newcastle Upon Tyne, United Kingdom; 2003.
12. Wang B, Panigrahi S, Tabil L, Crerar W. Effect of chemical treatment on mechanical and physical properties of flax fiber. Reinforced Rotationally Method Composites. In: ASAE Annual Meeting, Paper no. 046083. 2004.
13. Hussain AI, Abdel K, Ibrahim A. Effect of modified linen fibre waste on physio-mechanical properties of polar and non-polar rubber. Journal of Natural Science. 2010;8(8):82-89.
14. Mwaikambo LY, Ansell MP. Effect of chemical treatment on the properties of hemp, Sisal, Jute, and Kapok fibres for composites reinforcement. 2nd International Wood and Natural Fibre Composites Symposium, Kassel, Germany. 1999:1-6.
15. Abdelmonleh M, Bouti S, Belgacem MN, Duarte AP, Salah A.B, Gardini A. Modification of cellulosic fibres with functionalized silanes: Development of surface properties. International Journal of Adhesive 2004;24(1):43-54.
16. Kabir MM, Wang H, Aravinthan T, Cardona F, Lau KT. Effects of natural fibre surface on composite properties. Energy, Environment and Sustainability eddBE2011 Proceedings. 2011:94-99.
17. Mishra S, Mohanty AK, Drzal LT, Misra M, Parija S, NayakSK, Tipathy SS. Studies on mechanical performance of biofiber/glass reinforced polyester hybrid composites. Composite Science and Technology. 2003;63(10):1377-1385.
18. Bledzki AK, Gassan J. Composites reinforced with cellulose based fibres. Journal of Progress in Polymer Science. 1999;24(2):221-274.
19. Shaligram NS, Singh SK, Singhal RS, Szakacs G, Pandey A. Compactin production in solid-state fermentation using orthogonal array method by *P. brevicompactin*. BioChemical Engineering Journal. 2008;41(3):295-300.